

Nonlinear deep water waves: Theory and experiment

Henry C. Yuen and Bruce M. Lake

Citation: *Physics of Fluids (1958-1988)* **18**, 956 (1975); doi: 10.1063/1.861268

View online: <http://dx.doi.org/10.1063/1.861268>

View Table of Contents: <http://scitation.aip.org/content/aip/journal/pof1/18/8?ver=pdfcov>

Published by the *AIP Publishing*

Articles you may be interested in

[On weakly nonlinear modulation of waves on deep water](#)

Phys. Fluids **12**, 2432 (2000); 10.1063/1.1287856

[Experiments on capillary-gravity waves of solitary type on deep water](#)

Phys. Fluids **9**, 1963 (1997); 10.1063/1.869315

[Nonlinear standing waves: Theory and experiments](#)

J. Acoust. Soc. Am. **98**, 2753 (1995); 10.1121/1.413241

[Nonlinear slowly varying standing waves on deep water](#)

Phys. Fluids **27**, 2966 (1984); 10.1063/1.864582

[Comments on "Nonlinear deep water waves: Theory and experiment"](#)

Phys. Fluids **19**, 766 (1976); 10.1063/1.861540



Nonlinear deep water waves: Theory and experiment

Henry C. Yuen and Bruce M. Lake

Engineering Sciences Laboratory, TRW Systems, Redondo Beach, California 90278

(Received 21 October 1974; final manuscript received 25 March 1975)

The evolution and interaction of nonlinear wavepackets on deep water is studied both theoretically and experimentally. The nonlinear Schrödinger equation, first derived in this context by Hasimoto and Ono, is shown to be a special case of Whitham's theory. The exact solution to this equation predicts the existence of stable envelope solitons, which is indeed verified by laboratory experiments. A comparison between laboratory data and a numerical solution of the nonlinear Schrödinger equation is also given.

I. INTRODUCTION

The problem of the evolution and interaction of a nonlinear wavepacket on deep water has been a good test ground for many nonlinear wave theories developed in the past decade. It was studied by Lighthill¹ and Hayes² using Whitham's theory,³ and by Chu and Mei,⁴ Hasimoto and Ono,⁵ Davey and Stewartson⁶ using various multiple scales techniques. The results obtained via these two different approaches were not in total agreement.

In this paper, we re-examine the problem both theoretically and experimentally. We show that the nonlinear Schrödinger equation, first derived by Hasimoto and Ono⁵ in this context, is also a consequence of Whitham's theory when applied to the appropriate order. In other words, all the existing theories yield the same equation to the order considered, and earlier apparent discrepancies were merely the consequences of expansions to different orders. Next, we briefly summarize the predictions of Zakharov and Shabat's⁷ exact solution to the nonlinear Schrödinger equation, the most striking being the existence of envelope solitons. These predictions are then tested by carefully controlled laboratory experiments. Finally, some numerical results are presented to provide quantitative comparison between theory and experiment.

II. THE DERIVATION OF THE NONLINEAR SCHRÖDINGER EQUATION FROM WHITHAM'S THEORY

Whitham³ proposed that the evolution of a given system with Lagrangian $L(x, t)$ is described by the variation of the averaged Lagrangian:

$$\delta \int \int \mathcal{L} dx dt = 0, \quad (1)$$

where

$$\mathcal{L} = \frac{1}{2\pi} \int_0^{2\pi} L d\theta, \quad (2)$$

provided that the phase function θ exists. The characteristic frequency ω and wavenumber k are related to θ by

$$\theta_t = -\omega, \quad \theta_x = k.$$

For water waves it was shown by Luke⁸ that

$$L = \int_{-h_0}^{\eta} [\phi_t + \frac{1}{2}(\phi_x^2 + \phi_y^2) + gy] dy, \quad (3)$$

where h_0 is the depth of the fluid, η is the free surface, ϕ is the potential, g is the gravitational constant, and the density has been normalized to 1. For a weakly nonlinear, slowly varying, amplitude-modulated wavetrain, we can expand η as

$$\eta = a(\epsilon x, \epsilon t) \cos \theta + \frac{1}{2} k a^2(\epsilon x, \epsilon t) \cos 2\theta + \dots \quad (4)$$

The corresponding expansion for ϕ correct to $O(\epsilon, ka)$ is, in the case of infinite depth,

$$\phi = \frac{\omega a}{k} \sin \theta e^{ky} + \left[\frac{a_t}{k} \cos \theta + \frac{\omega a_x}{k^2} (1 - ky) \cos \theta \right] e^{ky} + \frac{\omega a^2}{2} \sin 2\theta e^{2ky} + \dots, \quad (5)$$

where the term containing $(1 - ky)$ is required to insure that ϕ satisfies Laplace's equation to the order considered. Substituting (4) and (5) into (3) and retaining terms of $O(\epsilon^2, k^2 a^2)$, we obtain

$$\begin{aligned} \mathcal{L} = & \frac{-\omega^2 a^2}{4k} + \frac{g a^2}{4} + \frac{a_t^2}{4k} + \frac{\omega a_x a_t}{4k^2} + \frac{\omega^2 a_x^2}{8k^3} + \frac{a a_{tt}}{2k} \\ & + \frac{3}{4} \frac{\omega a a_{xt}}{k^2} + \frac{3}{8} \frac{\omega^2 a a_{xx}}{k^3} + \frac{g k^2 a^4}{8}. \end{aligned} \quad (6)$$

Variation with respect to θ gives the energy equation

$$(a^2)_t + (C_g a^2)_x = 0, \quad (7)$$

where C_g is the linear group velocity

$$C_g = \frac{1}{2} \sqrt{g/k}. \quad (8)$$

Variation with respect to a gives the dispersion relation

$$\omega = \sqrt{gk} \left[1 + \frac{1}{2} k^2 a^2 + (a_{xx}/8k^2) \right]. \quad (9)$$

Note that in obtaining (9) we have made use of the leading order result of (7). Equations (7) and (9) are correct to $O(\epsilon^2, k^2 a^2)$. They are supplemented by the consistency equation

$$k_t + \omega_x = 0, \quad (10)$$

forming a closed set of equations for the evolution of ω , k , and a . This is a special case of Whitham's theory where we have assumed that the variations of ω and k are small compared with the variation of a . If this restriction is dropped, additional terms involving k_{xx} and $k_x a_x$ will occur. They can likewise be obtained by the above procedure, but the algebra is considerably more

complex.

Note that the only difference between the system of equations (7), (9), and (10) and that used by Lighthill¹ to study the evolution of a deep water wave pulse is the term $\sqrt{gk}(a_{xx}/8k^2)$ in the dispersion relation (9), which was neglected in his discussion. The absence of this $O(\epsilon^2)$ term makes Lighthill's system elliptic, and the solution he obtained becomes singular in a finite time. In fact, if we are only interested in obtaining this term from Whitham's theory, we can use an alternate and much simpler approach as shown in the Appendix.

To obtain the nonlinear Schrödinger equation, we let

$$\omega = \omega_0 + \tilde{\omega}, \quad k = k_0 + \tilde{k}, \quad (11)$$

where ω_0 and k_0 are constants. Correspondingly, the phase function θ takes the form

$$\theta = \theta_0 + \tilde{\theta}, \quad (12)$$

where

$$\theta_0 = k_0 x - \omega_0 t; \quad \tilde{\theta}_t = -\tilde{\omega}, \quad \tilde{\theta}_x = \tilde{k}. \quad (13)$$

This expansion assumes the existence of a constant "carrier wave," but in view of our neglect of k_{xx} , etc., terms, it is really not an additional restriction to the order considered.

Substituting (11) and (12) into (7), (9), and (10) and eliminating $\tilde{\omega}$ and \tilde{k} in favor of $\tilde{\theta}$, we obtain

$$a_t + \frac{1}{2}(\omega_0/k_0)a_x - (\omega_0/8k_0^2)(\tilde{\theta}_{xx} + 2\tilde{\theta}_x a_x) = 0, \quad (14)$$

$$\tilde{\theta}_t + \frac{1}{2}(\omega_0/k_0)\tilde{\theta}_x - (\omega_0/8k_0^2)[\tilde{\theta}_x^2 - (a_{xx}/a)] + \frac{1}{2}\omega_0 k_0^2 a^2 = 0. \quad (15)$$

If we introduce the complex variable $A = a e^{i\tilde{\theta}}$, (14) and (15) combine to become the nonlinear Schrödinger equation

$$i[A_t + \frac{1}{2}(\omega_0/k_0)A_x] - (\omega_0/8k_0^2)A_{xx} - \frac{1}{2}\omega_0 k_0^2 |A|^2 A = 0. \quad (16)$$

This equation was first discussed in the general context of weakly nonlinear, dispersive waves by Benney and Newell.⁹ It was first derived for water wave problems by Hasimoto and Ono.⁵

III. PREDICTIONS OF THE EXACT SOLUTION

Zakharov and Shabat⁷ showed that for initial conditions which approach zero sufficiently rapidly as $|x| \rightarrow \infty$ (corresponding to "pulses"), the nonlinear Schrödinger equation (16) can be solved exactly. The predictions of the exact solution in the context of water waves are interesting, and are summarized as follows:

(i) An initial wave envelope pulse of arbitrary shape will eventually disintegrate into a number of "solitons" and an oscillatory "tail." The number and structure of these solitons and the structure of the tail are completely determined by the initial conditions.

(ii) The tail is relatively small and unimportant for a pulse initial condition. It disperses linearly resulting in a $1/\sqrt{t}$ amplitude decay.

(iii) Each soliton is a permanent progressive wave solution of (16) in the form

$$S_n = a_n \operatorname{sech} \sqrt{2} k_0^2 a_n \left[(x - X_n) - \left(\frac{\omega_0}{2k_0} + v_n \right) t \right] \\ \times \exp \left\{ -\frac{i}{2} k_0^2 a_n^2 \omega_0 t - \frac{4ik_0^2}{\omega_0} v_n \left[(x - X_n) - \left(\frac{\omega_0}{2k_0} + v_n \right) t + \theta_n \right] \right\}, \quad (17)$$

where a_n and v_n characterize the amplitude and speed [relative to $C_{x0} = (\omega_0/2k_0)$] of the n th soliton, and X_n and θ_n represent its position and phase. Unlike the solitary wave solutions of the Korteweg-de Vries equation for shallow water,¹⁰ the amplitude a_n and speed v_n bear no direct relation to each other except that they are the imaginary and real parts of an associated scattering problem.

(iv) The solitons are stable in the sense that they can survive interactions with each other with no permanent change except a possible shift in position and phase (corresponding to a shift in the values of the constants X_n and θ_n).

(v) The time scale of formation of these solitons (i.e., the transition time from the initial to the asymptotic state) is in direct proportion to the length of the pulse, and in inverse proportion to the amplitude of the pulse.

(vi) For an initial pulse in which $\tilde{\omega}$ and \tilde{k} are small, we can roughly estimate the number of solitons n_s contained in it by the formula

$$n_s \doteq \frac{1}{\pi} \int \sqrt{2} k_0^2 a_0 f(x) dx, \quad (18)$$

where $A(x, 0) = a_0 f(x)$ is the initial profile with $0 \leq f(x) \leq 1$.

For detailed theoretical discussion of these properties, the reader is referred to the original work of Zakharov and Shabat.⁷

IV. EXPERIMENTAL RESULTS

We now test these predictions against experiments, which were performed in a 0.915 m \times 0.915 m \times 12.9 m water tank with a programmable surface wavemaker at one end and a wave-absorbing beach at the other. The tank facility (without the programmable wavemaker) is described in detail in Lewis *et al.*¹¹ The wavemaker is a hinged paddle activated by a hydraulic cylinder. The hydraulic system which drives the cylinder is controlled by a servoamplifier and feedback position transducer, so that the paddle motion is constrained to follow the waveform of the electronic signal applied at the input of the servoamplifier. The electronic input waveforms are prescribed by computer-generated analogue tape recordings. In this way, the particular initial waveforms of interest could be accurately produced in the wavetank for an amplitude range of 0.025 to 5.0 cm (peak-to-peak) and for a frequency range from 1 to 5 Hz. The evolution of each initial waveform was then measured using capacitance wave amplitude gauges at stations 1.53, 3.05, 4.58, 6.10, 7.63, and 9.15 m downstream of the wavemaker. The gauge outputs were linearly proportional to wave amplitude, with sensitivities typically 1.2 V/cm over a 5 cm range.

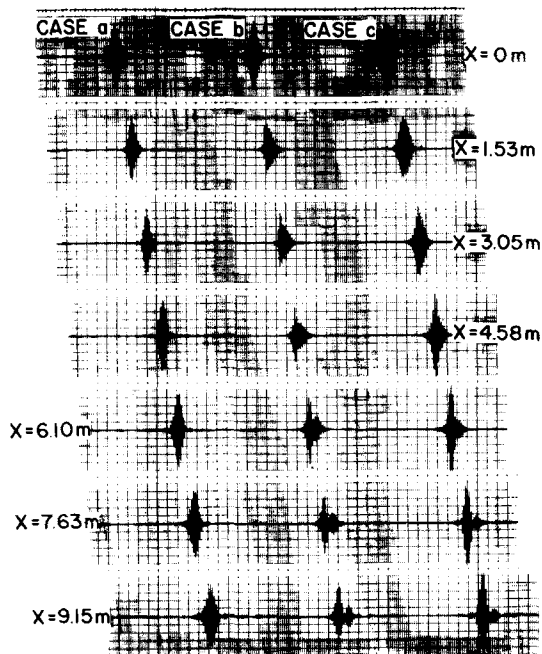


FIG. 1. Evolution of wave pulses. Case A, initial pulse with soliton profile, $\omega_0 = 2$ Hz, initial $(ka)_{\max} \approx 0.14$. Case B, initial pulse with sech profile and amplitude twice that for soliton profile, $\omega_0 = 2$ Hz, amplitude scale of traces reduced by factor of 2.5 compared with cases A and C. Case C, initial pulse with sine profile and amplitude equal to that for soliton profile, $\omega_0 = 2$ Hz, initial $(ka)_{\max} \approx 0.14$. In all figures, time increases from left-to-right and the $x = 0$ m traces show initial wave pulse inputs to the wavemaker.

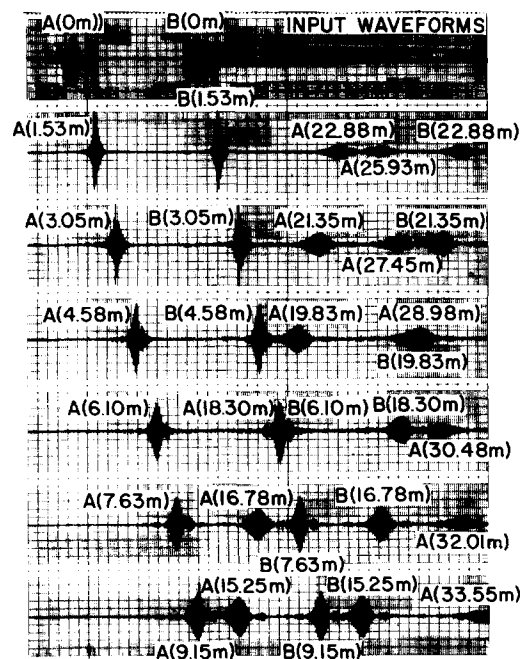


FIG. 2. Head-on collision of two wave pulses. The initial conditions for each pulse are the same as for the high frequency pulse in Fig. 3, $\omega_0 = 3$ Hz, initial $(ka)_{\max} \approx 0.2$. Noted on this figure are the propagation distances for wave pulses A and B during the process.

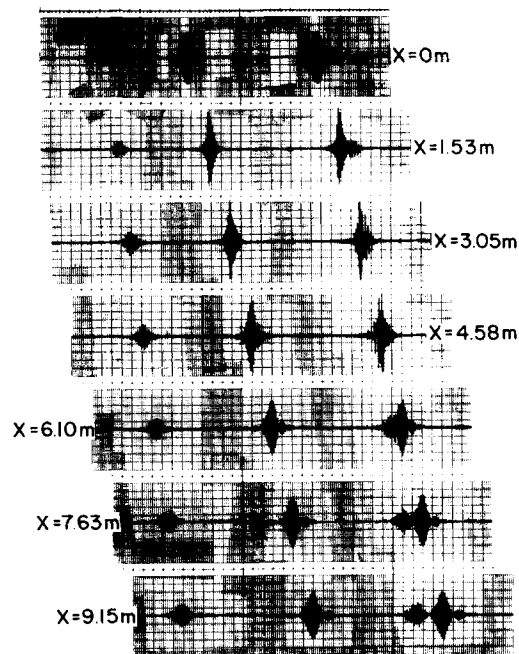


FIG. 3. One wave pulse overtaking and passing through another wave pulse. Left-hand trace: first pulse alone, $\omega_0 = 1.5$ Hz, initial $(ka)_{\max} \approx 0.01$, six-cycle pulse. Center trace: second pulse alone, $\omega_0 = 3$ Hz, initial $(ka)_{\max} \approx 0.2$, 12-cycle pulse which disintegrates into two solitons. Right-hand traces: interaction of the two pulses.

Although the output of every amplitude gauge was linearly proportional to wave amplitude, each gauge had a slightly different sensitivity. In recording the measurements shown in Figs. 1–3, the effects of these sensitivity differences, together with the first-order effects of viscous dissipation, have been removed by adjusting the amplifier gain on each oscillograph channel so that the amplitude channel outputs were equal when measuring a linear sinusoidal wavetrain as it propagated down the tank. A 2-Hz wavetrain was used to match the amplitude scales for the measurements shown in Fig. 1 and a 3-Hz wavetrain was used for the measurements shown in Figs. 2 and 3.

The measurements shown in Figs. 1–3 illustrate the qualitative comparison between our experimental observations and the phenomena predicted by the exact solution. Figure 1 shows the evolution of three pulses which have approximately the same effective duration but different initial profiles. Each pulse has the same carrier frequency $\omega_0 = 2$ Hz. Case A (the left-hand traces) is a soliton profile which obeys the height-to-width relationship (17). Case B (the center traces, shown on an amplitude scale reduced by a factor of 2.5 compared with cases A and C), is a sech profile with amplitude twice that of the soliton profile. Case C is a sine profile with the same amplitude as the soliton profile. Case C and the first two measurements in case B are similar to results obtained in pulse experiments performed by Feir.¹² In cases B and C the initial profiles break into solitons, while in case A, where the initial profile is already that of a soliton, relatively little happens. This series of experiments confirms the theoretical predic-

tion that an initial pulse profile disintegrates into solitons and a tail, except when it is itself a perfect soliton as in case A. The slight distortion in the profiles of case A is attributed to the fact that the wavemaker action is not entirely equivalent to initial conditions posed at $t=0$, but rather a time profile posed at $x=0$.

Figure 2 shows the head-on collision of two pulses of the same carrier frequency, $\omega_0 = 3$ Hz. It is accomplished by reflecting the first pulse off a vertical end wall (the wave-absorbing beach was removed) before sending in the second. The pulses were generated with the same amplitude, frequency, and pulse shape at $x=0$. After generating the pulses, the wave paddle was left in a vertical position so that the pulses would reflect from a vertical end wall at $x=0$ m as well as at $x=12.19$ m. The numbers shown on the wave records in the figure identify the propagation distances for wave pulses A and B during the process. The solitons and their formation processes show little effect of interaction, as can be seen by comparison of pairs of profiles such as A(7.63 m) (no collision) and B(7.63 m) (one collision) or A(21.35 m) (one collision) and B(21.35 m) (two collisions). This verifies the interaction properties predicted by the theory. No attempts have been made to measure the phase shifts quantitatively, but judging from the data they are very small for all the cases we have observed.

Figure 3 shows the interaction of two pulses of different carrier frequencies. The first is a 3.0-Hz pulse which propagates more slowly than the second, a 1.5-Hz pulse. The left-hand traces in the figure show the evolution of the 1.5-Hz pulse alone. The center traces show the evolution of the 3.0-Hz pulse alone. By the time it reaches $x=9.15$ m, the 3.0-Hz pulse has evolved into two solitons. The right-hand traces show the evolution and interaction of the two pulses when the 3-Hz pulse is generated ahead of the 1.5-Hz pulse at $x=0$ m. As they propagate, the two pulses pass through one another and emerge in reversed order by $x=9.15$ m. Note that despite the long and rather violent interaction they have undergone, the two pulses emerge practically unaffected as can be seen by comparison with the results where each evolves in the absence of the other. Strictly speaking, this type of interaction between pulses of different carrier wave frequencies cannot be described by a single equation such as Eq. (16). However, it has been shown by Oikawa and Yajima¹³ that solitons with different carrier frequencies also survive interactions with no permanent change other than position and phase shifts. The governing equations for these multiwave systems can likewise be obtained by Whitham's method by use of more than one phase function.

Predictions concerning the time scales of formation have been verified. The estimate for the number of solitons is also in good agreement with experiments. For example, (18) would predict $n_s = 2$ and $n_s = 3$, respectively, for cases B and C of Fig. 1. Additional experiments with longer initial pulse lengths were performed and, using reflective tank end walls, we have observed disintegration into as many as eight solitons. In cases involving reflections from vertical end walls, it should

be noted that we do not yet have a theoretical justification for reflective invariance, although the experiments strongly indicate that the pulses are unaffected by such reflections.

V. NUMERICAL COMPUTATION

To further assess the degree of agreement between theory and experiment, we have solved (16) numerically by a modified Crank-Nicholson scheme. Details of the scheme will be discussed in a later paper. The case we wish to report here corresponds to case C of Fig. 1. The initial condition for the program is constructed by fitting the data recorded by the wave gauge at $x=1.53$ m. Since the leading order effect of dissipation has been scaled out by the gauge calibrations for the profiles in Fig. 1, we have compared the computed profiles directly with the recorded profiles without additional adjustments in amplitudes. The results are shown in Fig. 4. All the characteristics of the large soliton are very well predicted. Predictions of the detailed structures of the two smaller solitons are less accurate. It is seen that the amplitude of the leading soliton is overpredicted, and there appears to be a mismatch of its stage of evolution (the experimental data seem to indicate a more complete separation from the main soliton). These discrepancies may be attributed to the various approximations involved in the theory, the major ones being:

- (i) Curve fitting of recorded profile at $x=1.53$ m for initial condition;
- (iii) Neglect of second-order dissipative effects due

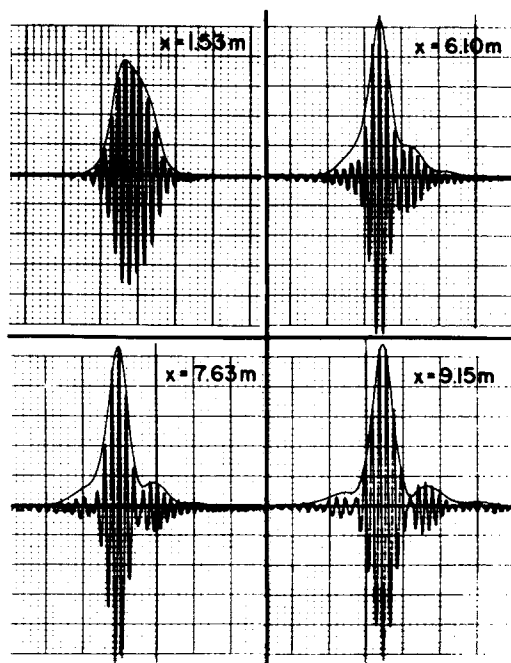


FIG. 4. Comparison of numerical computation with experimental data. The case considered corresponds to case C in Fig. 1. The computed results (shown as envelope curves) are superposed on the oscillograph traces from the experiment. The curve at $x=1.53$ m is the input to the numerical computation, and the other curves show comparison with data at three downstream stations.

to nonlinearity of the equation; and

(iii) Neglect of higher-order terms in ϵ and ka in the derivation of (16).

In fact, in view of these approximations, the agreement shown in Fig. 4 may actually be better than one might justifiably expect.

VI. CONCLUSIONS

We have shown that by carrying out the averaged variational principle to a higher order as indicated by Whitham,³ we are able to obtain the nonlinear Schrödinger equation which was first derived by Hasimoto and Ono⁵ and was generally thought to be unobtainable from Whitham's theory. We have examined the consequences of the exact solutions obtained by Zakharov and Shabat⁷ in the context of water waves and have verified them by experiment. We have also shown that the equation is quantitatively satisfactory by comparing laboratory data to numerically computed results.

ACKNOWLEDGMENTS

We would like to thank Professor P. G. Saffman for his valuable advice crucial to the development of the theory.

This research was supported by the Applied Physics Laboratory of Johns Hopkins University under contract APL/JHU No. 600102.

APPENDIX: ALTERNATE DERIVATION OF THE DISPERSION RELATION (9)

Whitham³ showed that for a weakly nonlinear system the averaged Lagrangian always takes the form

$$\mathcal{L} = a^2 G(\omega, k) + a^4 G_2(\omega, k), \quad (\text{A1})$$

where $G(\omega, k) = 0$ is the linear dispersion relation. To take into account the slow space-time variation of a , we consider ω and k as pseudo-differential operators and

expand

$$\omega \approx \bar{\omega} + \epsilon \frac{\partial}{\partial T}, \quad k \approx \bar{k} + \epsilon \frac{\partial}{\partial X}, \quad (\text{A2})$$

where $X = \epsilon x$, $T = \epsilon t$, and $a = a(X, T)$. If these are substituted into (A1) and Taylor-expanded, we have

$$\begin{aligned} \mathcal{L} = & a^2 G(\bar{\omega}, \bar{k}) + \frac{\epsilon^2}{2} [G_{\omega\omega}(\bar{\omega}, \bar{k}) a_T^2 + 2G_{\omega k}(\bar{\omega}, \bar{k}) a_T a_X \\ & + G_{kk}(\bar{\omega}, \bar{k}) a_X^2] + a^4 G_2(\bar{\omega}, \bar{k}). \end{aligned} \quad (\text{A3})$$

For deep water waves, $G(\omega, k) = \omega^2 - gk$. The present level of argument will not give the value for $G_2(\omega, k)$, but we can identify it as the nonlinear correction, being $\frac{1}{2}k^2\omega$. In any case, $G_2(\omega, k)$ does not affect the outcome of the $O(\epsilon^2)$ term we proposed to obtain. Variation of (A3) with respect to a then gives us the correct dispersion relation (9). Note again that $\bar{\omega}$, \bar{k} need not be constants, but their variations have been assumed small compared to those of a .

¹M. J. Lighthill, *J. Inst. Math. Appl.* 1, 269 (1965); *Proc. R. Soc. A* 299, 28 (1967).

²W. D. Hayes, *Proc. R. Soc. A* 320, 187 (1970); 320, 209 (1970); 338, 101 (1974).

³G. B. Whitham, *Proc. R. Soc. A* 283, 238 (1965); *J. Fluid Mech.* 22, 273 (1965); *J. Fluid Mech.* 27, 339 (1967); *Proc. R. Soc. A* 299, 6 (1967); *J. Fluid Mech.* 44, 373 (1970).

⁴V. H. Chu and C. C. Mei, *J. Fluid Mech.* 41, 873 (1970); *J. Fluid Mech.* 47, 337 (1971).

⁵H. Hasimoto and H. Ono, *J. Phys. Soc. Jap.* 33, 805 (1972).

⁶A. Davey and K. Stewartson, *Proc. R. Soc. A* 338, 101 (1974).

⁷V. E. Zakharov and A. B. Shabat, *Zh. Eksp. Teor. Fiz.* 61, 118 (1971) [*Sov. Phys.—JETP* 34, 62 (1972)].

⁸J. C. Luke, *J. Fluid Mech.* 27, 395 (1967).

⁹D. J. Benney and A. C. Newell, *J. Math. Phys.* 46, 133 (1967).

¹⁰H. Segur, *J. Fluid Mech.* 59, 721 (1973); J. L. Hammack and H. Segur, *ibid.* 65, 289 (1974).

¹¹J. Lewis, B. M. Lake, and D. R. S. Ko, *J. Fluid Mech.* 63, 773 (1974).

¹²J. E. Feir, *Proc. R. Soc. A* 299, 54 (1967).

¹³M. Oikawa and N. Yajima, *J. Phys. Soc. Jap.* 37, 486 (1974).